Processing Shape, Motion and Three-dimensional Shape-from-motion in the Human Cortex

Scott O. Murray, Bruno A. Olshausen and David L. Woods[1]

Center for Neuroscience, University of California at Davis, Davis, CA 95616 and [1]Department of Neurology, VA Medical Center, 150 Muir Road (127 A), Martinez, CA 94553, USA

Shape and motion are complementary visual features and each appears to be processed in unique cortical areas. However, object motion is a powerful cue for the perception of three-dimensional (3-D) shape, implying that the two types of information — motion and form — are well integrated. We conducted a series of fMRI experiments aimed at identifying the brain regions involved in inferring 3-D shape from motion cues. For each subject, we identified regions in occipital–temporal cortex that were activated when perceiving: (i) motion in unstructured random-dot patterns, (ii) 2-D and 3-D line drawing shapes, and (iii) 3-D shapes defined by motion cues (shape-from-motion, SFM). We found closely adjacent areas in the lateral occipital region activated by random motion and line-drawing shapes. In addition, we found that the SFM stimuli produced a greater MRI signal in only one of the areas identified with the random motion and line-drawing stimuli: the superior lateral occipital (SLO) region. High-resolution analysis showed that SFM objects and line drawings were processed in separate but adjacent sub-regions in SLO, suggesting that SLO codes object shape but retains topographic segregation based on shape cues. Expanding the analysis to the entire cortex identified a parietal area that had overlapping activation for both SFM and line drawings and increased MRI signal for 3-D versus 2-D shapes, suggesting this area is important for processing shape information.

Introduction

The visual system forms representations of many properties of the environment including information about the shapes of objects and their motion. Shape and motion are features with seemingly complementary properties. Inferring object shape involves detecting spatial relationships among features that are generally assumed to be fixed relative to one another. For example, when the angles of distant corners are in alignment, the visual system is able to infer that the space between them forms a single shape, whether the shape is moving or stationary. Inferring object motion, by contrast, involves solving a temporal correspondence problem in which a set of features at one point in time are matched with another set of features at a later point in time. For example, if the trajectories of many points are consistent with a single global rotation about a common axis in 3-D, then we perceive a single rotational motion in 3-D as opposed to a collection of independently moving points (Siegel and Andersen, 1988).

The complementary quality of shape and motion appears to be reflected in the organization of the visual system (Ungerleider and Mishkin, 1982). In the human visual system, certain cortical areas, such as area MT+, appear to be specialized for processing motion (Zeki *et al.*, 1991; Tootell *et al.*, 1995; Sunaert *et al.*, 1999). Others, such as the lateral occipital complex (LOC), are important for processing object shape (Malach *et al.*, 1995; Kanwisher *et al.*, 1996). Activity in this region increases when images of objects are viewed compared to scrambled versions of the same objects [see Grill-Spector *et al.* (Grill-Spector *et al.*, 2001) for review].

Despite the seemingly complementary nature of shape and motion, the two features are closely linked. Motion, for example, is an important cue for identifying object boundaries (Julesz, 1971; Braddick, 1974) in everyday vision, and tracking shape features over time is the basis of motion computation. Indeed, shape-from-motion stimuli (SFM) using random-dot patterns demonstrate that motion information alone can create vivid 3-D shape perceptions (Wallach and O'Connell, 1953; Koenderink and Van Doorn, 1986; Siegel and Andersen, 1988; Treue *et al.*, 1991). Given that there are specialized areas for processing motion and shape, the question arises as to how and where motion and form information is brought together. It is possible that a subset of neurons in the motion system process shape information (Malonek *et al.*, 1994; Buracas and Albright, 1996; Kourtzi *et al.*, 2002) or, alternatively, motion information could be passed to shape-processing neurons in lateral occipital regions (Grill-Spector *et al.*, 1998). Also, regions outside overtly visual areas could be responsible for integrating shape and motion information (Oram and Perret, 1996).

The studies presented here use functional MRI to examine these questions in several steps. First, we presented moving random dot patterns and line drawings to identify motion and shape processing regions. Then, we examined modulations in these regions caused by SFM stimuli. Finally, we performed a supplementary analysis comparing activations caused by the SFM and line-drawing stimuli in regions outside visual cortex.

Materials and Methods

Subjects and Stimuli

Nine right-handed individuals participated in the experiments and each was scanned in a single imaging session. Stimuli were presented with a PC running *Presentation* software (www.neurobs.com) through a Sharp LCD projector onto a rear-projection screen located at the feet of the subjects. The screen was viewed with an angled mirror positioned on the head-coil with a viewing angle of 11 × 10°.

Retinotopic Mapping

Subjects viewed two types of retinotopic mapping stimuli. The first were counter-phase (8 Hz) checkerboard wedges of 12° located at the horizontal and vertical meridians. These served to map boundaries between visual areas (Sereno *et al.*, 1995; Engel *et al.*, 1997). The second were foveal (2° diameter) and peripheral (9°) counter-phase (8 Hz) annuli that served to map the retinotopic extent of each area (Sereno *et al.*, 1995; Engel *et al.*, 1997). Two retinotopic mapping scans were performed – one that alternated the horizontal and vertical meridian stimuli and one that alternated the foveal and peripheral ring stimuli. In both scans, stimuli were presented in 20 s blocks with seven alternations between conditions.

Motion

To identify motion-processing areas, a single scan was performed in

which three types of stimuli were presented: (i) randomly moving dots, (ii) flickering dots, and (iii) stationary dots. Each block lasted 20 s and there were six presentations of each condition. The randomly moving dots consisted of an array of 450 dots subtending 10° of visual angle. Each dot moved in a random direction with constant speed (4°/s). The motion displays were generated by creating movie sequences with each frame stored as a separate bitmap. The sequence played forward then reversed so that random motion was continually observed. To promote eye fixation and to equate attentional demands across conditions, subjects were asked to detect randomly occurring, brief (60 ms) luminance increases of the fixation cross. For the baseline stationary condition, a randomly chosen frame from the movie sequence was presented along with the same fixation luminance-detection task.

To separate responses due purely to temporal aspects of the motion stimulus, signal associated with a flickering display was compared to that produced by random motion stimuli. The use of flicker maintains temporal properties but does not have the same spatio-temporal structure of motion. Flicker stimuli were generated by randomizing the order of the movie frames used for the motion stimuli and were presented with the same fixation luminance-detection task.

Shape

To identify shape-processing regions, three conditions were presented over two scans: (i) random lines, (ii) lines that formed 2-D shapes and (iii) lines that formed 3-D shapes (Fig. 1). (The first two subjects scanned did not view the 2-D shape condition.) Each condition was presented in 30 s blocks and presented a total of eight times over the two scans. To control for potential differences in attention subjects responded with a button press to brief (100 ms), randomly occurring global luminance reductions (40%) in the stimuli in all conditions. The 2-D shapes were generated by randomly selecting 4–7 vertices at a minimum distance from fixation and connecting the vertices. The random lines were created by breaking the 2-D shapes at their intersections and randomly repositioning them while maintaining the same mean distance (4°) from fixation. The 3-D shapes were the same as the 2-D shapes in all respects with the addition of small extensions that added perceived depth (Fig. 1). Each figure was presented for 750 ms.

Shape-from-motion

Random-dot displays were presented under three conditions: (i) stationary dots, (ii) 'velocity-scrambled' moving dots and (iii) projections of a random-dot pattern onto moving three-dimensional geometric shapes (shape-from-motion, SFM) (Fig. 2). Conditions were presented in 30 s blocks and presented a total of eight times over two imaging scans. The stimuli in each condition contained 450 dots and subtended 10°. The dots in the shape-from-motion (SFM) stimuli were projections of rigid, transparent, geometric shapes including a cube, cylinder and 'house-shaped' figures. These three shapes were used because they had limited confounding shape cues. Many SFM shapes (e.g. pyramid) have additional shape cues created by the border of the stimuli (triangle). Dots were randomly selected from a uniform distribution on the object surface and kept fixed relative to the rotating object surface and orthographically projected onto the image plane. The dots were rotated on a randomly chosen 3-D axis for 40° in 1.5° increments. The dots did not have limited lifetimes. A dot on the front surface of an object moving in one direction eventually appeared on the back surface moving in the opposite direction. Each stimulus presentation lasted 890 ms followed by 110 ms blank-screen delay before the next stimulus presentation. The perception of shape in the SFM stimuli is created by the distribution of relative speed that is perceived as differing depths by the visual system (motion parallax). Examples of the SFM stimuli and the control stimuli (described below) can be viewed at http://redwood.ucdavis.edu/scott/research/sfm.

The SFM stimuli were compared to velocity-scrambled stimuli – these had the same velocities (direction and speed) as the SFM stimuli but were randomly reassigned to different dots creating perceptually random motion, similar to Siegel and Andersen (Siegel and Andersen, 1988). The first frame from a SFM stimulus also served as the first frame in the corresponding velocity-scrambled condition. The baseline, stationary dot condition presented a randomly chosen frame from the SFM stimuli. As with the line drawing stimuli, subjects were asked to detect brief (100 ms), randomly occurring luminance reductions (40%) in the stimuli.

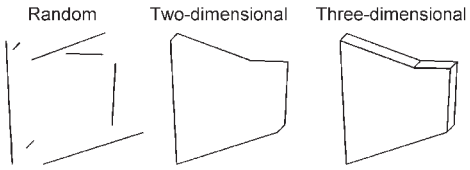

Figure 1. Examples of the stimuli used to analyze shape processing. Actual figures were white lines on a black background subtending, on average, 8° of visual angle.

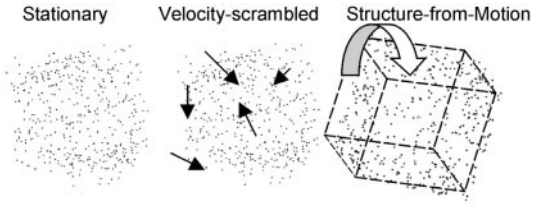

Figure 2. Examples of the stimuli used to analyze structure-from-motion (SFM) processing. Actual figures were white dots on a black background subtending 9° of visual angle. The velocity-scrambled stimuli had identical velocities as the SFM stimuli but were randomly re-assigned to different dots creating perceptually random motion. (The dashed line and arrows are added for illustration.) Movie demonstrations of the stimuli can be viewed at http://redwood.ucdavis.edu/scott/research/sfm/.

MRI Acquisition

For all the experiments, scanning was done on a 1.5 T Marconi scanner at the Northern California Veterans Administration Health Care System in Martinez, California. Standard imaging procedures (T_E = 40 ms; flip angle = 90°, T_R = 2000 ms) were used. Data were collected from 20 5 mm thick axial slices (128 × 128, FOV = 240 mm) that, for most subjects, covered the entire brain. To aid in visualization of statistical maps and to more easily define visual areas, data were projected onto inflated cortices using FreeSurfer (Dale and Sereno, 1993; Dale *et al.*, 1999; Fischl *et al.*, 1999, 2001) using high-resolution spin-echo anatomical scans collected from each subject (FOV = 240 mm, matrix = 256 × 212 × 256, T_E = 4.47 ms, T_R = 15 ms, flip angle = 35).

Data Analysis

The data were pre-processed using SPM99 (www.fil.ion.ucl.ac.uk/spm), including realignment of functional scans to correct for head motion, normalization into standardized coordinates, and spatial smoothing (4 mm^3 FWHM kernel). Statistical maps were generated for each subject using SPM99 and served as a basis for defining regions-of-interest (ROIs). In all of the analyses described below, unless otherwise mentioned, an ROI was defined as a contiguous region of voxels surpassing a minimum statistical threshold of $P < 10^{-3}$. To calculate percent change, we first derived the linearly detrended time course of the MR signal intensity for each voxel in an ROI. The average percent signal change was then calculated for each stimulus type, relative to the average signal intensity during a baseline condition. Baseline conditions differed for different analyses and are described below. Because the fMRI response typically lags 4–6 s after the neural response, the first image in each epoch was assigned to the condition of the preceding epoch and we omitted the next two images from analysis (i.e. ignored transition images between epochs). Since no hemispheric differences were observed, if an ROI was present in both hemispheres (e.g. left and right MT+), the data were averaged together. Paired two-tailed *t*-tests were used to compare percent change data between conditions. No correction for multiple voxelwise comparisons was used because the data were analyzed within ROIs that had been defined.

Motion Analysis

Motion ROIs were defined by a comparison of activations in stationary and random moving dot conditions. Because many visual areas are

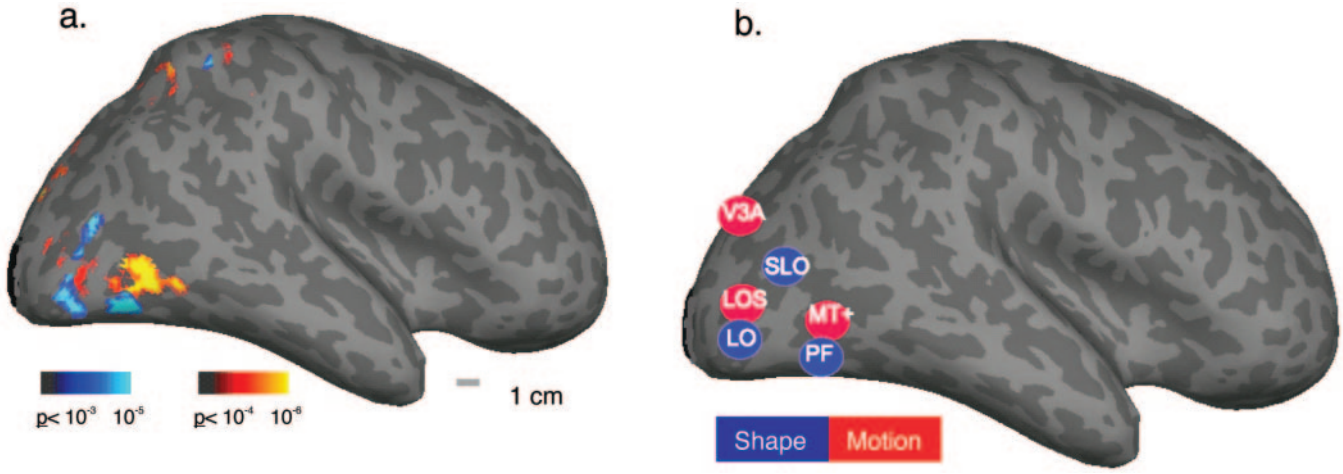

Figure 3. (*a*) Data are from a single subject displayed on the inflated cortex of the right hemisphere. The yellow/red color-map shows areas of increased activity in response to motion stimuli compared with stationary stimuli. The blue color-map shows areas of increased activity to 3-D line drawings compared with random lines (parietal cortex activity is presented in detail in later figures). (*b*) A schematic showing the relative locations of motion areas (red) including visual area 3A (V3A), lateral occipital sulcus (LOS), and middle temporal area (MT+) and shape areas (blue) including superior lateral occipital (SLO), lateral occipital (LO) and posterior fusiform (PF).

sensitive to dynamic stimuli such as motion (whether or not they are actually 'motion areas'), a higher statistical criterion was used, $P < 10^{-4}$. For the flicker versus random motion ROI analysis, the stationary dot condition served as the baseline condition from which percent change was calculated.

Shape Analysis

ROIs involved in processing shape were defined as those voxels with more signal to 3-D lines than random lines. Subsequent analyses, such as comparisons between 2-D and 3-D perception, were done with these predefined ROIs. In these analyses, the random line condition served as the baseline; thus, percent changes reflect differences from the random line condition.

Shape-from-motion Analysis

SFM processing was first analyzed by considering only those ROIs identified with the static 3-D line drawings and the random motion stimuli, with the stationary dot condition serving as a baseline for percent change calculations. Subsequent to the ROI analysis, a standard mapping analysis was performed comparing SFM and the velocity-scrambled stimuli. For this, statistical maps were generated for each subject and significant changes were defined as $P < 10^{-3}$.

Results

Motion Perception

The yellow/red color-map in Figure 3*a* shows typical activations associated with random dot motion. The comparison revealed several regions of increased signal with the largest being an area located in the middle temporal area corresponding to MT+. In addition, we observed consistent increases in signal in an area posterior and superior to MT+, an area previously described as LOS (lateral occipital sulcus) and in area V3A (Tootell *et al.*, 1997; Orban *et al.*, 1999; Sunaert *et al.*, 1999). The locations of these three areas (MT+, LOS and V3A) are summarized in a schematic in Figure 3*b*. Primary visual cortex (V1, not visible on Fig. 3) also showed consistent increases in signal in response to moving dots.

It is possible that neurons in an area that increase their activity in response to moving versus stationary dots are simply responding to the temporal properties of the motion stimulus rather than to movement itself. This was addressed by comparing motion stimuli (dynamic stimuli with spatial structure) to flicker

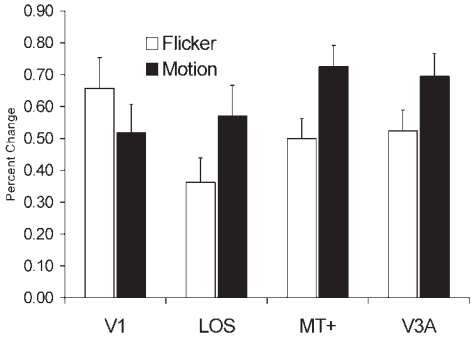

Figure 4. The average percent signal change of motion areas from a baseline of stationary dots comparing motion and flicker stimuli. All extra-striate motion areas show significant increases in activity ($P < 10^{-3}$) for motion versus flicker stimuli. V1 shows a significant ($P < 10^{-3}$) decrease in activity in response to motion versus flicker.

stimuli (dynamic stimuli without spatial structure). Similar to Sunaert *et al.* (Sunaert *et al.*, 1999), we found significant increases in response to motion stimuli compared to flicker stimuli in all three motion areas (Fig. 4). However, we observed a significant *decrease* in activation in V1, also consistent with previous imaging studies [e.g. Sunaert *et al.* (Sunaert *et al.*, 1999)] as well as physiological and modeling studies (Qian and Andersen, 1994; Qian *et al.*, 1994).

Shape Perception

The blue color-map in Figure 3*a* shows several regions of increased signal to 3-D line drawing stimuli compared to randomized lines. Other studies of shape perception have referred to a lateral occipital 'complex' meaning that multiple areas within this region show increases in activation to shapes relative to non-shapes (Malach *et al.*, 1995; Grill-Spector *et al.*, 1998, 1999). We observed discrete and consistent areas of activation and have chosen to label these regions individually. The locations of these individual areas had a reliable relationship to the identified motion processing areas making identification easier across subjects. Figure 3*b* shows a summary schematic of these regions (blue) and their positions relative to motion areas (red). We have labeled the more posterior and ventral region as LO as it closely matches the location described in the original

Table 1
Talairach coordinates (Talairach and Tournoux, 1988) for the center of each ROI

	Left			Right		
	x	y	z	x	y	z
LOS	–27 ± 5	–91 ± 5	8 ± 12	34 ± 4	–88 ± 5	4 ± 12
V3A	–19 ± 6	–91 ± 6	24 ± 3	21 ± 7	–90 ± 6	22 ± 6
MT+	–45 ± 3	–73 ± 4	5 ± 6	48 ± 3	–66 ± 3	2 ± 5
LO	–39 ± 4	–82 ± 2	–2 ± 5	41 ± 4	–81 ± 6	2 ± 3
SLO	–33 ± 6	–82 ± 5	15 ± 5	37 ± 7	–78 ± 4	12 ± 5
PF	–43 ± 7	–70 ± 2	–7 ± 7	45 ± 4	–65 ± 3	–8 ± 8

Values represent the mean ± SD in mm.

study identifying a lateral occipital object-processing region (Malach *et al.*, 1995). As can be seen from Figure 3, LO and the motion-area LOS are located very closely to each other. We labeled an area superior to LO as SLO. Previous studies [e.g. Grill-Spector *et al.* (Grill-Spector *et al.*, 1998)] have referred to a dorsally located object processing area near V3A and it is possible that this area corresponds to the area we have labeled SLO.

We also consistently observed an area of increased signal immediately inferior to area MT+, which we refer to as PF (posterior fusiform). Our differentiation between LO and PF follows Grill-Spector *et al.* (Grill-Spector *et al.*, 1999). They distinguished two areas – one referred to as LO and a second more anterior region they termed posterior fusiform/lateral occipital anterior (PF/LOa). PF/LOa, in their study, was less affected by changes in image properties such as position and illumination than LO. Based on the described anatomical location, PF/LOa may be the same region we labeled PF. Table 1 summarizes the locations of motion and shape areas across all of the subjects studied.

The three shape-processing ROIs were tested for their response to 2-D and 3-D shapes. All increased in response to the 3-D shapes in comparison to the 2-D shapes (Fig. 5), consistent with the previous finding that the LOC is processing three-dimensional structure (Moore and Engel, 2001). However, other research [e.g. Kourtzi and Kanwisher (Kourtzi and Kanwisher, 2000)] did not find a difference in LOC activation for 3-D versus 2-D shapes. Further studies will be necessary to test the degree to which depth information is coded within the LOC.

Shape-from-motion

Signal Increases

The motion areas defined by random dot motion (MT+, LOS and V3A) and shape areas defined by static 3-D line drawings (LO, SLO and PF) as well as V1 were included in the ROI analysis comparing signal to the SFM stimuli and the velocity-scrambled stimuli. This analysis assumes that the same network of cortical regions involved in processing static line drawings and random motion will be involved in processing SFM. As can be seen from Figure 6, area SLO was the only area with a significant increase to the SFM stimuli relative the velocity-scrambled stimuli. Because SLO was defined by its response to 3-D line drawings, it suggests this region is involved in integrating 3-D shape information from multiple cues (motion and edges). In addition, SLO was the only lateral occipital region with a strong preference for 3-D compared to 2-D drawings (Fig. 5), suggesting a unique importance for representing 3-D shape information.

The ROI approach to analyzing SFM perception is a statistically sensitive test of the hypothesis that SFM perception will

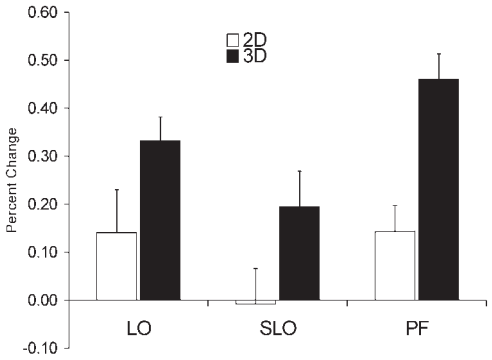

Figure 5. Average percent signal change of shape areas to 2-D and 3-D figures calculated from a baseline of random lines. Areas LO and PF show significant changes from the baseline random-line condition for the 2-D figures and all three areas show significant increases comparing 3-D to 2-D figures.

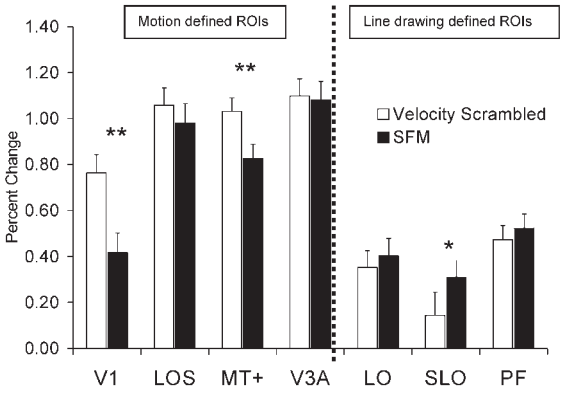

Figure 6. Average percent signal change for ROIs comparing the random (velocity-scrambled) stimuli to SFM, calculated from a baseline of the stationary condition. Only area SLO showed a significant ($P < 10^{-2}$) increase in activity for the SFM stimuli. Both MT+ and V1 showed significant ($P < 10^{-3}$) decreases in activity.

involve the modulation of cortical areas involved in processing static shapes and random motion. However, it unnecessarily restricts the regions analyzed because it would overlook regions uniquely activated by SFM. For this reason, we generated statistical maps (*P* values for every voxel) comparing signal in the SFM condition versus the velocity-scrambled control condition for each subject. Eight of the nine subjects had an area of activation to the SFM stimuli that was adjacent (slightly posterior and superior) to SLO defined by static 3-D line drawings. To characterize the relative distribution of SFM and line drawing activation around SLO, the location of the voxel with the highest

signal change (activation peak) was determined for SFM and 3-D line drawings. This was done in each hemisphere for each subject where there was SLO activation to both the line drawing and SFM stimuli. Each dimension (x (medial–lateral), y (anterior–posterior), z (dorsal–ventral) was then compared with a paired two-tail t-test. A significant ($P < 0.05$, d.f. = 12) difference was observed in the z direction with the SFM peak located dorsal to the 3-D line drawing peak. There was also a nearly significant ($P < 0.07$, d.f. = 12) trend for a posterior shift in the SFM peak.

To visualize the topographic differences, the coordinates of the SFM activation peaks were subtracted from the 3-D line drawing activation peaks and plotted (Fig. 7*c*). The differences are also evident when overlaying statistical maps from the two conditions (Fig. 7*b*). The results suggest that while there is considerable overlap in SLO for line-drawing and SFM activation, there may be sub-regions in SLO specialized for processing the two types of stimuli.

There were other consistent activations in response to the SFM stimuli outside visual cortex. All subjects showed increases to the SFM stimuli relative to the velocity-scrambled stimuli in the mid-lateral parietal cortex. Average Talairach coordinates were –34 ± 5, –49 ± 7 and 58 ± 3 mm for the left hemisphere, and 35 ± 8, –47 ± 4 and 59 ± 6 mm for the right hemisphere. Statistical maps derived from SFM activation (SFM versus velocity-scrambled) were compared with statistical maps derived from 3-D line drawings (3-D versus random). Calculating the activation peaks in the two conditions and using the same method as for SLO (Fig. 8) revealed no significant difference in the two conditions (Fig. 8*b*), raising the possibility that this parietal area may be important for shape perception. We defined an ROI based on the comparison of SFM versus velocity-scrambled stimuli and analyzed the response to 2-D and 3-D line drawings. Figure 9 shows that this area has a significantly larger response to 3-D versus 2-D line drawings, a pattern similar to areas within the LOC (compare with Fig. 5). This strongly suggests this area is involved in shape perception and we have tentatively labeled it the parietal shape area (PSA). Based on anatomical location and functional characteristics, this area likely corresponds to the cIPS region recently described by James *et al.* (James *et al.*, 2002).

Signal Decreases

In contrast to the increases in signal observed in SLO and the PSA, MT+ and V1 showed significant decreases in signal in response to the SFM stimuli compared to the velocity-scrambled condition (Fig. 6). These reductions are unlikely to be caused by simple low-level differences in the stimuli. Stimulus luminance, dot number, and dot velocities were equated between these conditions. However, though a given SFM stimulus has many directions and speeds, in general, it has two (opposite) directions of motion when analyzed at a local scale. This could affect activity in MT+ in two different ways. First, even though the same velocities are present in the SFM and velocity-scrambled stimuli, there is higher *local* motion coherence (percentage of dots moving in the same direction) in the SFM condition relative to the velocity-scrambled condition. The higher local coherence would have been expected to *increase* MT+ activity for the SFM stimuli (Britten *et al.*, 1992; Rees *et al.*, 2000). Second, there is higher motion opponency (local motions in the opposite direction) in the SFM stimuli and this would have been expected to *decrease* activity in MT+ (Heeger *et al.*, 1999). However, neither motion opponency (Heeger *et al.*, 1999) nor motion coherence (Rees *et al.*, 2000; Braddick *et al.*, 2001) has been shown to affect V1 activity.

Discussion

Shape and Motion Processing

The lateral occipital 'complex' is generally identified functionally as voxels located in the lateral occipital and posterior/middle temporal cortices with increased signal to images of objects compared with non-objects (Malach *et al.*, 1995; Grill-Spector *et al.*, 1998, 1999). In this study we reliably differentiated three areas within the LOC: LO, SLO and PF. These areas had a consistent relationship to identified motion areas, facilitating their identification across subjects. The relationship between motion and shape areas is similar to the results of a previous study (Braddick *et al.*, 2000). They found two areas of activation in response to form perception that likely correspond to the areas we labeled LO and SLO, each with neighboring motion-processing areas. The close proximity of shape and motion areas points to the importance of pre-defining subject-specific regions-of-interest in studies examining shape and motion processing. For example, it would be difficult to distinguish activations in LO or LOS without first predefining their locations.

Shape-from-motion

Lateral Occipital Regions

In attempting to determine how SFM is processed by the visual system, we first independently identified 'motion areas' using random dot motion and 'shape areas' using static line-drawings and asked which of these ROIs showed differences in signal to SFM versus velocity-scrambled stimuli. The only ROI in occipital and temporal cortices with significantly increased signal to the SFM stimuli compared to the velocity-scrambled stimuli was area SLO. Given that SLO was defined by its increased signal to static line drawing shapes and had increased signal to the SFM stimuli, the data suggest that SLO may be important for integrating shape and motion cues. However, it is not possible to conclude that SLO is a cue-independent shape processing area for two reasons. First, it is possible that individual neurons within SLO are cue-specific with overlapping distributions that are not easily differentiable using fMRI. It may be possible to determine whether there is true cue-independence within SLO in future studies by using recently developed fMRI adaptation techniques (Grill-Spector *et al.*, 1999; Kourtzi and Kanwisher, 2000; Grill-Spector and Malach, 2001). Indeed, the results from the mapping analysis (identifying voxels throughout the entire cortex active to SFM compared to the velocity-scrambled stimuli) also called into question whether the SLO was cue-independent. This analysis showed that the distributions of activation in response to SFM stimuli and 3-D line drawing stimuli were different within the SLO region. While there was overlap, in most subjects the peak SFM activation was located superior and/or posterior to the line-drawing defined peak, suggesting there may be cue-dependent sub-regions.

The choice of stimuli may have affected the response patterns we observed. For example, only three different SFM shapes (with multiple axes of rotation) were used. The shapes were chosen because any static view carried little or no shape information – that is, there were very limited shape cues due to dot distribution. However, the reduced number of shapes may have led to overall reduced LOC activity. Previous studies have shown that lateral occipital regions adapt to repeated

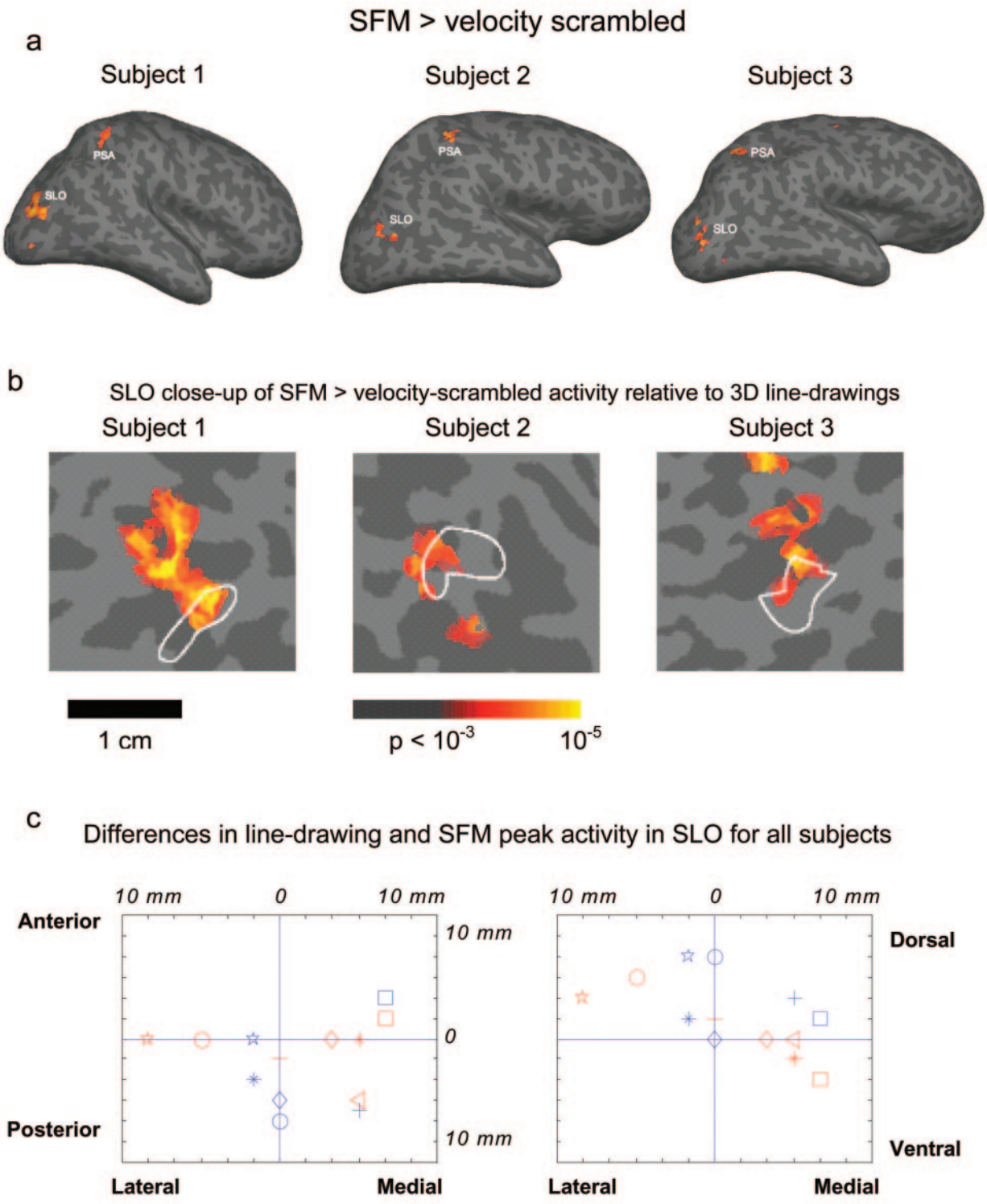

Figure 7. (*a*) Statistical maps comparing SFM and velocity-scrambled stimuli on the inflated right hemispheres of three subjects. (*b*) Close-up views of SFM activity in SLO from the same subjects. The white outline shows the $P < 10^{-3}$ boundary of activity comparing static 3-D line drawings and random lines. While there is considerable overlap, there is a posterior and/or dorsal shift in the SFM activity. (*c*) The activation peak (x, y, z coordinates) for the line drawing and SFM stimuli were subtracted in each hemisphere for every subject. Each point represents the position of the SFM peak relative to the line drawing peak. Each hemisphere and subject is a single point with its own color/symbol that correspond in the two plots. The left plot shows the medial/lateral versus anterior/posterior distribution and the right plot shows the medial/lateral versus dorsal/ventral distribution.

presentations (Grill-Spector *et al.*, 1999; Kourtzi and Kanwisher, 2000). Therefore, it is possible that if LOC subregions have differential adaptation rates (e.g. if ventral areas such as PF and LO adapt more quickly than SLO), it could have produced the pattern of results we observed. Similarly, it is possible that, instead of SLO being specialized for SFM, the choice of shapes

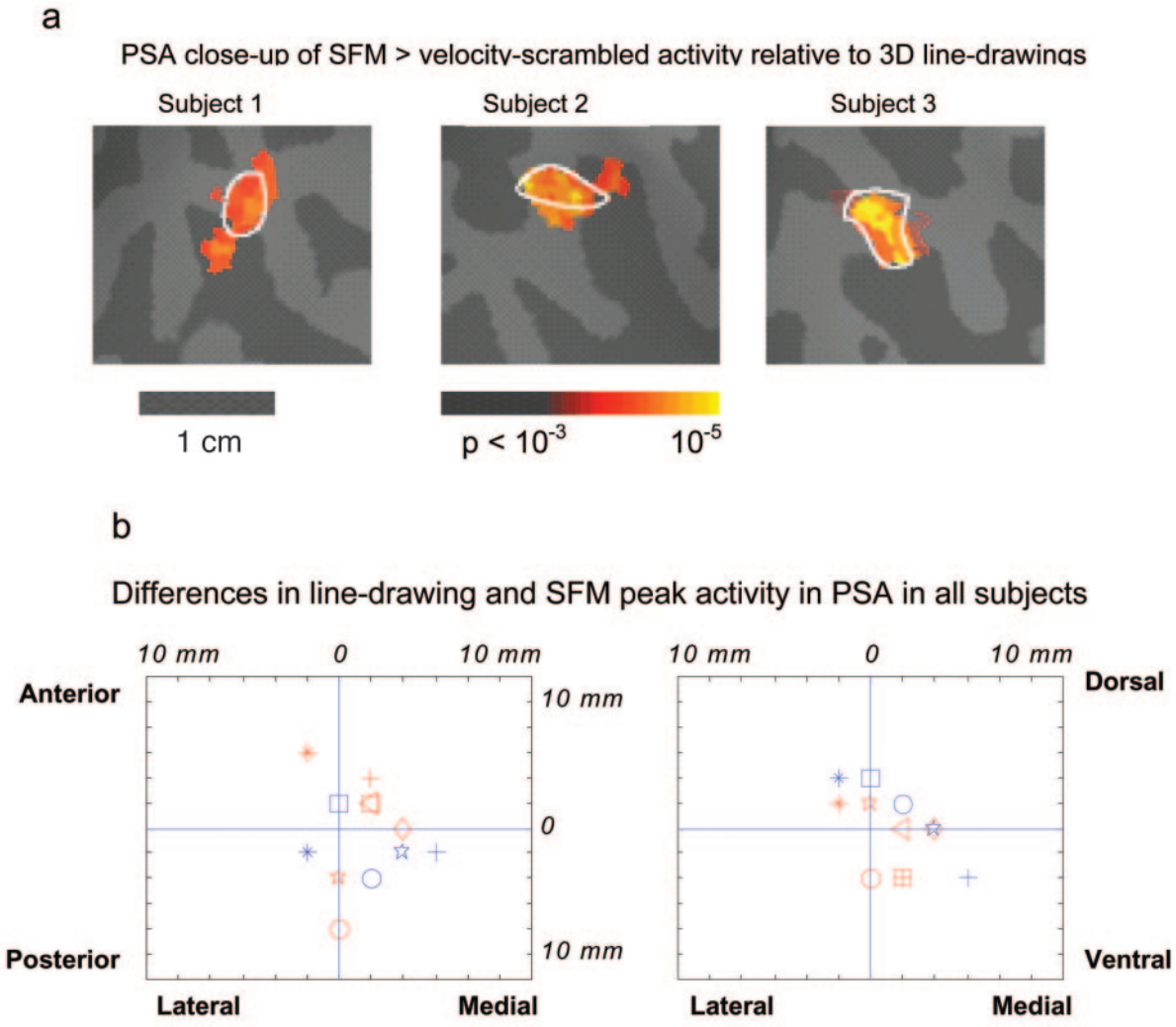

Figure 8. (*a*) Activation maps from the same three subjects in Figure 7 comparing SFM and velocity-scrambled stimuli in the PSA. The white outline shows the $P < 10^{-3}$ boundary of activity comparing static 3-D line drawings and random lines. While there are small differences between SFM and line drawings in the extent of activation, the positions are highly overlapping. (*b*) The same method as Figure 7*c* was used to compare activation peaks for the line drawing and SFM stimuli. There is no consistent difference in the location of activation peaks in the two conditions in the PSA.

was not optimal for driving activity in ventral lateral occipital regions (LO and PF) relative to SLO.

Our conclusions are different than those of Grill-Spector *et al.* (Grill-Spector *et al.*, 1998). They showed considerable overlap in LOC for shapes defined by motion contours and luminance contours. However, there were also small differences in their signal distributions. In addition, motion contours are a very different shape cue than 3-D SFM and it may be that LOC neurons are more invariant to shapes defined by luminance and motion contours, both of which are extracted at the level of V1 (Lamme *et al.*, 1993; Reppas *et al.*, 1997).

The results reported here differ somewhat with those of a previous fMRI study examining SFM perception comparing the perception of a curved surface versus random motion and rotational motion (Paradis *et al.*, 2000). They found increased signal in V3A in response to SFM and no consistent differences in MT+ or V1, with some subjects demonstrating significant increases and others significant decreases. Because subjects were allowed to passively view the stimuli, the authors discuss the possible influences of stimulus-specific subject attention on their results. Along similar lines, in early pilot studies we found that including an attention-demanding task increased the consistency of our results.

V1 and MT+

In contrast to the signal increases we observed in SLO, there were significant signal decreases in V1 and MT+ for the SFM stimuli relative to the velocity-scrambled stimuli. Previous explanations suggest that grouping velocities into a single object reduces the need to signal individual local velocities in V1 and MT+ (Murray *et al.*, 2002). In that study, functional MRI was used to measure activations in higher object processing areas and in V1 and MT+ in response to visual elements (line segments and motion vectors) that were either grouped into objects or randomly arranged. Significant signal increases were observed in LOC as well as concurrent reductions of activity in V1 and MT+ when elements formed coherent shapes, suggesting that activity in early visual areas is reduced as a result of grouping processes performed in higher areas.

It is important to emphasize that a decrease in MT+ signal does not imply a lack of involvement in the computations necessary for SFM perception, especially in light of recent functional

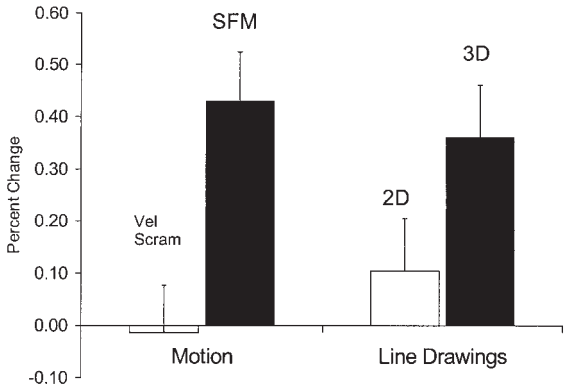

Figure 9. Activity in the PSA to motion and line drawings. The PSA showed a significant increase in activity to SFM stimuli compared to the velocity-scrambled stimuli. In addition, this area showed increases to 3-D versus 2-D line drawings similar to areas that comprise the LOC (compare with Fig. 5).

imaging (Orban *et al.*, 1999), neurophysiological (Bradley *et al.*, 1998), and modeling results (Buracas and Albright, 1996). It does appear that responses in MT are non-linear and highly dependent on the nature of the motion percept. For example, single unit experiments in macaques have shown that opposite motion directions suppress MT responses, but that the suppression decreases when opposite directions are shown at different disparities (Bradley *et al.*, 1995; Snowden *et al.*, 1991). In addition, Bradley *et al.* (Bradley *et al.*, 1998) demonstrate that activities in monkey MT neurons are correlated with spontaneous reversals of perceived surface order in a SFM display, even though the stimulus remained identical. Thus, one possible explanation for reduced MT+ signal is that there is a strong tendency to perceive only one direction of motion in the SFM stimuli – the axis of rotation – despite the presence of many individual local directions of motion (which are very apparent in the velocity-scrambled stimuli). The reduced signal in MT+ may reflect the perceived reduction in the number of motion directions. Also, what is missing from the current data is *when* the signal in MT+ is decreasing. Previous research (Siegel and Andersen, 1988; Treue *et al.*, 1991) has demonstrated that SFM perception is a dynamic process, requiring a high degree of temporal integration. It is possible that activity in MT+ is high before or during initial surface assignments, and then is reduced for the remaining portion of the stimulus as other regions begin to represent the stimulus. The net effect in the fMRI signal may be reduced activity. Future research should focus on the dynamics of SFM processing within areas such as MT+.

Parietal Cortex

The mapping analysis also identified a region in the parietal cortex, the PSA, which may be an important site for integrating shape information across different cues. There were only small differences in the location of peak signal in response to the SFM and line-drawing stimuli and the PSA showed increased signal to 3-D relative to 2-D figures similar to the LOC. Other imaging studies of shape perception have explained parietal activations as the result of attentional confounds, i.e. that object perceptions engage a subject's attention more than non-objects (Kourtzi and Kanwisher, 2000). While the parietal cortex is undoubtedly involved in attention (Corbetta *et al.*, 1995; Wojciulik and Kanwisher, 1999), it is unlikely that PSA activation in the current study was the result of an attentional artifact as subjects' attention was focused on a difficult luminance-change detection task in all conditions. Further evidence that PSA activation was not due to an attentional confound was that there was no difference in signal between the velocity-scrambled motion condition and the baseline stationary condition, despite moving stimuli being more 'engaging' than stationary stimuli.

Neurophysiological studies have also indicated a role of the parietal cortex in shape processing (Sereno and Maunsell, 1998) and the parietal cortex may be important for processing depth cues, such as shading (Humphrey *et al.*, 1996) or surface slant (Sakata *et al.*, 1997). Also, the PSA is located in the approximate region of AIP (Culham and Kanwisher, 2001), an area important for visually guided grasping. Passive viewing of graspable objects (e.g. tools) activates regions near AIP (Chao and Martin, 2000), and having detailed representations of object shape would clearly be important for guiding the motor system (Goodale and Milner, 1992). In fact, a recent study by James *et al.* (James *et al.*, 2002) showed that a parietal cortex region similar in location to the PSA showed no priming to depth-rotated images of objects whereas ventral object processing regions did show priming. In other words, parietal object processing areas seem to treat rotated images as new objects – consistent with the role of parietal areas in object-directed action. This is consistent with our finding of apparent cue-invariance in the PSA where overall shape is important for guiding the motor system but the specific cue is not.

Our finding of multiple shape processing regions in temporal and parietal cortex is consistent with a recent fMRI study in monkeys examining shape perception (Sereno *et al.*, 2002). However, in their study, they found a multitude of areas in occipital, temporal, parietal and frontal cortices as well as overlapping activations to several shape cues including SFM, shading and silhouettes. It is possible that the difference in the number of active areas is a result of species differences or could somehow be attributable to the use of anesthetized animals. Regardless, the results of Sereno *et al.* (Sereno *et al.*, 2002) and our current results point out that regions well outside established visual cortex are involved in three-dimensional shape perception.

Conclusions

The current experiments show that there are distinct but adjacent regions within the human visual cortex for processing shape and motion stimuli with anatomical relationships that were consistent across subjects. The superior lateral occipital region (SLO) was the only visual cortical area with increased signal in response to 3-D shapes defined by motion (SFM) and 3-D line drawings. Further analyses suggest that SFM may be processed in a dorsal/posterior sub-region of SLO. In addition, an area in the parietal cortex – the PSA – may play a role in forming cue-independent representations of object shape, and indicates that areas outside well-established visual areas may be important for processing multiple object shape cues.

Notes

Address correspondence to Scott Murray, Center for Neuroscience, University of California at Davis, Davis, CA 95616, USA. Email: somurray@ucdavis.edu

References

Braddick OJ (1974) A short range process in apparent motion. Vision Res 14:519–527.

Braddick OJ, O'Brien JMD, Wattam-Bell J, Atkinson J, Turner R (2000) Form and motion coherence activate independent, but not dorsal/ventral segregated, networks in the human brain. Curr Biol 10:731–734.

Braddick OJ, O'Brien JM, Wattam-Bell J, Atkinson J, Hartley T, Turner R

(2001) Brain areas sensitive to coherent visual motion. Perception 30:61–72.
Bradley DC, Qian N, Andersen RA (1995) Integration of motion and stereopsis in middle temporal cortical area of macaques. Nature 16:609–611.
Bradley DC, Chang GC, Anderson RA (1998) Encoding of three-dimensional structure-from-motion by primate area MT neurons. Nature 392:714–717.
Britten KH, Shadlen MN, Newsome WT, Movshon JA (1992) The analysis of visual motion: a comparison of neuronal and psychophysical performance. J Neurosci 12:4745–4765.
Buracas GT, Albright TD (1996) Contribution of area MT to perception of three-dimensional shape: a computational study. Vision Res 36: 869–887.
Chao LL, Martin A (2000) Representation of manipulable man-made objects in the dorsal stream. Neuroimage 12:478–484.
Corbetta M, Shulman GL, Miezin FM, Petersen SE (1995) Superior parietal cortex activation during spatial attention shifts and visual feature conjunction. Science 270:802–805.
Culham JC, Kanwisher NG (2001) Neuroimaging of cognitive functions in human parietal cortex. Curr Opin Neurobiol 11:157–163.
Dale AM, Sereno MI (1993) Improved localization of cortical activity by combining EEG and MEG with MRI cortical surface reconstruction: a linear approach. J Cogn Neurosci 5:162–176.
Dale AM, Fischl B, Sereno MI (1999) Cortical surface-based analysis I: segmentation and surface reconstruction. Neuroimage 9:179–194.
Engel SA, Glover GH, Wandell BA (1997) Retinotopic organization in human visual cortex and the spatial precision of functional MRI. Cereb Cortex 7:181–192.
Fischl B, Sereno MI, Dale AM (1999) Cortical surface-based analysis II: inflation, flattening, a surface-based coordinate system. NeuroImage, 9:195–207.
Fischl B, Liu A, Dale AM (2001) Automated manifold surgery: constructing geometrically accurate and topologically correct models of the human cerebral cortex. IEEE Trans Med Imaging 20:70–80.
Goodale MA, Milner AD (1992) Separate visual pathways for perception and action. Trends Neurosci 15:20–25.
Grill-Spector K, Malach R (2001) fMR-adaptation: a tool for studying the functional properties of human cortical neurons. Acta Psychol (Amst) 107:293–321.
Grill-Spector K, Kushnir T, Edelman S, Itzchak Y, Malach R (1998) Cue-invariant activation in object-related areas of the human occipital lobe. Neuron 21:191–202.
Grill-Spector K, Kushnir T, Edelman S, Avidan G, Itzchak Y, Malach R (1999) Differential processing of objects under various viewing conditions in the human lateral occipital complex. Neuron 24: 187–203.
Grill-Spector K, Kourtzi Z, Kanwisher N (2001) The lateral occipital complex and its role in object recognition. Vision Res 2001 41: 1409–1422.
Heeger DJ, Boynton GM, Demb JB, Seidemann E, Newsome WT (1999) Motion opponency in visual cortex. J Neurosci 19:7162–7174.
Humphrey GK, Symons LA, Herbert AM, Goodale MA (1996) A neurological dissociation between shape from shading and shape from edges. Behav Brain Res 76:117–125.
James TW, Humphrey GK, Gati JS, Menon RS, Goodale MA (2002) Differential effects of viewpoint on object-driven activation in dorsal and ventral streams. Neuron 35:793–801.
Julesz B (1971) Foundations of cyclopean perception. Chicago, IL: University of Chicago Press.
Kanwisher N, Chun MM, McDermott J, Ledden PJ (1996) Functional imagining of human visual recognition. Brain Res Cogn Brain Res 5:55–67.
Koenderink JJ, Van Doorn AJ (1986) Depth and shape from differential perspective in the presence of bending deformations. J Opt Soc Am Ser A 3:242–249.
Kourtzi Z, Kanwisher N (2000) Cortical regions involved in perceiving object shape. J Neurosci 20:3310–3318.
Kourtzi Z, Bulthoff HH, Erb M, Grodd W (2002) Object-selective responses in the human motion area MT/MST. Nat Neurosci 2002 5:17–18.
Lamme VAF, Van Dijk BW, Spekreijse H (1993) Contour from motion processing in primary visual cortex. Nature 363:541–543.
Malach R, Reppas JB, Benson RR, Kwong KK, Jiang H, Kennedy WA, Ledden PJ, Brady TJ, Rosen BR, Tootell RBH (1995) Object-related activity revealed by functional magnetic resonance imaging in human occipital cortex. Proc Natl Acad Sci USA 92:8135–8139.
Malonek D, Tootell RBH, Grinvald A (1994) Optical imaging reveals the functional architecture of neurons processing shape and motion in owl monkey area MT. Proc R Soc Lond B 258:109–119.
Moore C, Engel SA (2001) Neural response to perception of volume in the lateral occipital complex. Neuron 29:277–286.
Murray SO, Kersten D, Olshausen BA, Schrater P, Woods DL (2002) Shape perception reduces activity in human primary visual cortex. Proc Natl Acad Sci USA 99:15164–15169.
Oram MW, Perret DI (1996) Integration of form and motion in the anterior superior temporal polysensory area (STPa) of the macaque monkey. J Neurophysiol 76:109–129.
Orban GA, Sunaert S, Todd JT, Hecke PV, Marchal G (1999) Human cortical regions involved in extracting depth from motion. Neuron 24:929–940.
Paradis AL, Cornilleau-Peres V, Droulez J, Van De Moortele PF, Lobel E, Berthoz A, Le Bihan D, Poline JB (2000) Visual perception of motion and 3-D structure from motion: an fMRI study. Cereb Cortex 10:772–783.
Qian N, Andersen RA (1994) Transparent motion perception as detection of unbalanced motion signals II. Physiology. J Neurosci 14:7367–7380.
Qian N, Andersen RA, Adelson EH (1994) Transparent motion perception as detection of unbalanced motion signals. III. Modeling. J Neurosci 14:7381–7392.
Rees G, Friston K, Koch C (2000) A direct quantitative relationship between the functional properties of human and macaque V5. Nat Neurosci 3:716–723.
Reppas JB, Niyogi S, Dale AM, Sereno MI, Tootell RBH (1997) Representation of motion boundaries in retinotopic human visual cortical areas. Nature 388:175–179.
Siegel RM, Andersen RA (1988) Perception of three-dimensional structure from motion in monkey and man. Nature 331:259–261.
Snowden RJ, Treue S, Erickson RG, Andersen RA. (1991) The response of area MT and V1 neurons to transparent motion. J Neurosci 11: 2768–2785.
Sakata H, Taira M, Kusunoki A, Tanaka Y (1997) The parietal association cortex in depth perception and visual control of hand action. Trends Neurosci 20:350–357.
Sereno AB, Maunsell JHR (1998) Shape selectivity in primate lateral intraparietal cortex. Nature 395:500–503.
Sereno MI, Dale AM, Reppas JB, Kwong KK, Belliveau JW, Brady TJ, Rosen BR, Tootell RBH (1995) Borders of multiple visual areas in humans revealed by functional magnetic resonance imaging. Science 268:889–893.
Sereno ME, Trinath T, Augath M, Logothetis NK (2002) Three-dimensional shape representation in monkey cortex. Neuron 33:635–652.
Sunaert S, Hecke PV, Marchal G, Orban GA (1999) Motion-responsive regions of the human brain. Exp Brain Res 127:355–370.
Tootell RBH, Reppas JB, Kwong KK, Malach R, Born RT, Brady TJ, Rosen BR, Belliveau JW (1995) Functional analysis of human MT and related visual cortical areas using magnetic resonance imaging. J Neurosci 15:3215–3230.
Tootell RBH, Mendola JD, Hadjikhani NK, Ledden PJ, Liu AK, Reppas JB, Sereno MI, Dale AM (1997) Functional analysis of V3A and related areas in human visual cortex. J Neurosci 17:7060–7078.
Treue S, Husain M, Andersen RA (1991) Human perception of structure from motion. Vision Res 31:59–75.
Ungerleider, LG, Mishkin M (1982) Two cortical visual systems. In: The analysis of visual behavior (Ingle DJ, Mansfield RJW, Goodale MA, eds), pp. 549–586. Cambridge, MA: MIT Press.
Wallach H, O'Connell DN (1953) The kinetic depth effect. J Exp Psychol 45:205–217.
Wojciulik E, Kanwisher N (1999) The generality of parietal involvement in visual attention. Neuron 23:747–764.
Zeki S, Watson JDG, Lueck CJ, Friston KJ, Kennard C, Frackowiak RSJ (1991) A direct demonstration of functional specialization in human visual cortex. J Neurosci 11:641–649.